Introduction to Robotics

Lecture 3

Shuang Li, Jianwei Zhang
[sli, zhang]@informatik.uni-hamburg.de

University of Hamburg
Faculty of Mathematics, Informatics and Natural Sciences
Department of Informatics
Technical Aspects of Multimodal Systems

April 23, 2021

Outline

Outline (cont.)

Recapitulation of DH-Parameter

- universal minimal robot description
- based on frame transformations
- four parameters per frame transformation
- serial chain of transformations
- unique description of T_6

Drawbacks

- ambiguous convention
- only kinematic chain described
- missing information on geometry, physical constraints, dynamics, collisions, inertia, sensors, . . .

Definition of joint coordinate systems

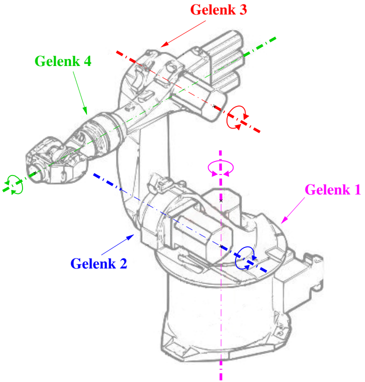

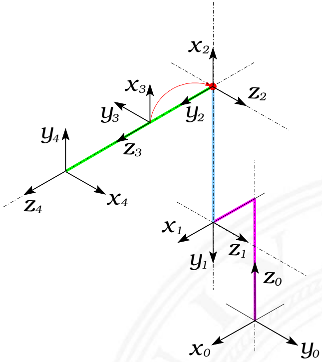

- CS_0 is the stationary origin at the base of the manipulator
- axis z_{i-1} is set along the axis of motion of the i^th joint
- axis x_i is the common normal of $z_{i-1} \times z_i$
- axis y_i concludes a right-handed coordinate system

Parameters for description of two arbitrary links

Two parameters for the description of the link structure i

- a_i : shortest distance between the z_{i-1}-axis and the z_i-axis
- α_i : rotation angle around the x_i-axis, which aligns the z_{i-1}-axis to the z_i-axis

a_i and α_i are constant values due to construction

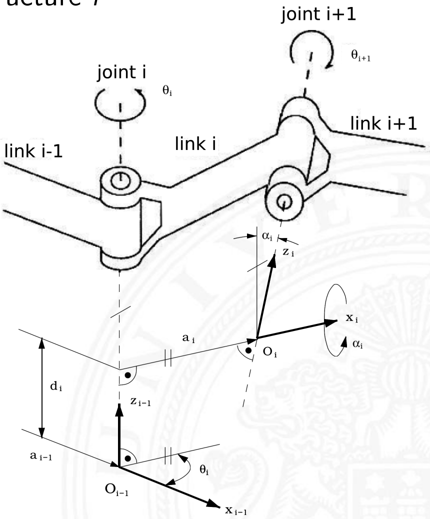

Parameters for description of two arbitrary links (cont.)

Two for relative distance and angle of adjacent links

- d_i : distance origin O_{i-1} of the $(i\text{-}1)^{st}$ CS to intersection of z_{i-1}-axis with x_i-axis
- θ_i : joint angle around z_{i-1}-axis to align x_{i-1}- parallel to x_i-axis into x_{i-1}, y_{i-1}-plane

θ_i and d_i are variable

- rotational: θ_i variable, d_i fixed
- translational: d_i variable, θ_i fixed

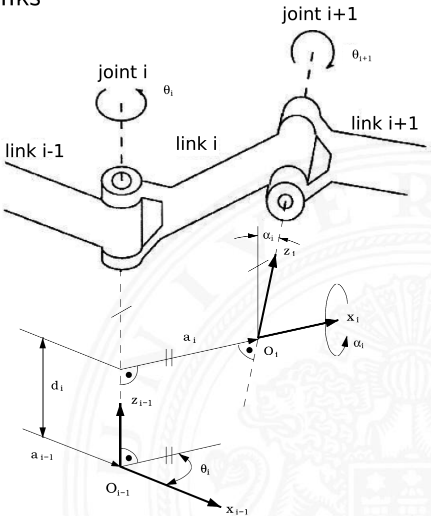

Example featuring PUMA 560

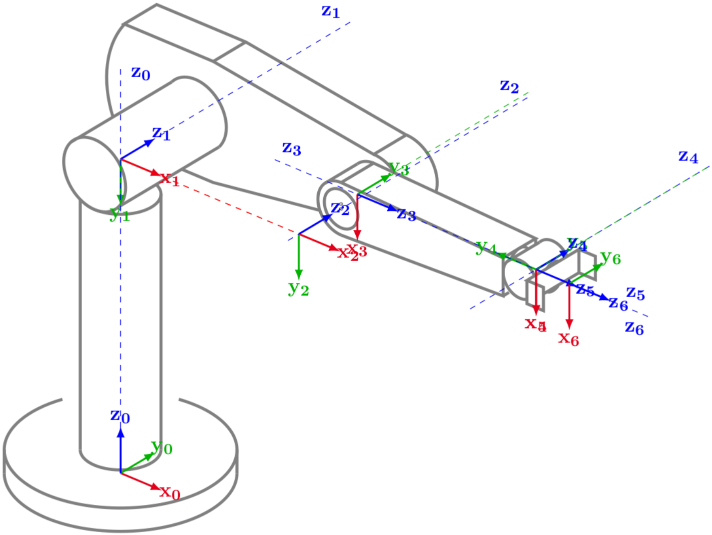

Example featuring PUMA 560

DH parameters of PUMA 560

Joint	a_i	α_i	d_i	θ_i
1	0	$-\frac{\pi}{2}$	d_1	θ_1^*
2	a_2	0	0	θ_2^*
3	a_3	$\frac{\pi}{2}$	d_3	θ_3^*
4	0	$-\frac{\pi}{2}$	d_4	θ_4^*
5	0	$\frac{\pi}{2}$	0	θ_5^*
6	0	0	d_6	θ_6^*

In order to transfer the manipulator-endpoint into the base coordinate system, T_6 is calculated as follows:

Universal Robot Description Format

Documentation

http://wiki.ros.org/urdf
http://wiki.ros.org/urdf/XML
http://wiki.ros.org/urdf/Tutorials

- robot description format used in ROS[19]
- hierarchical description of components
- XML format representing robot model
  - kinematics and dynamics
  - visual
  - collision
  - configuration

[19] http://ros.org

URDF: XML Tree Structure

- 1^{st}-level structure

```
<robot name="samplerobot">
</robot>
```

- 2^{nd}-level structure

  `link`, `joints`, `sensors`, `transmissions`, `gazebo`, `model_state`

- 3^{rd}-level structure

  `visual`, `inertia`, `collision`, `origin`, `parent`, ...

- 4^{th}-level structure

  ⋮

URDF: XML Tree Structure (cont.)

- Filename: robotname.urdf
- XML prolog:

```
<?xml version="1.0" encoding="utf-8"?>
```

- XML element types

```
<tag attribute="value"/>
```

```
<tag attribute="value">
text or element(s)
</tag>
```

- XML comments

```
<!-- Comments are placed within these tags -->
```

URDF: Link

Link describes geometrical properties of a rigid body.

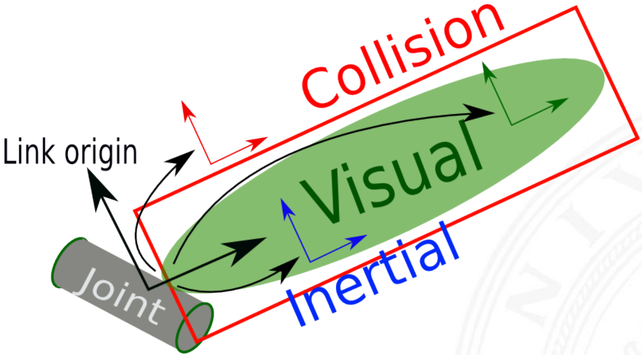

20

URDF: Link (cont.)

```
<link name="sample_link">
<!-- describes the mass and inertial properties of
the link -->
<inertial/>

<!-- describes the visual appearance of the link.
can be described using geometric primitives or
meshes -->
<visual/>

<!-- describes the collision space of the link.
is described like the visual appearance -->
<collision/>
</link>
```

[20] http://wiki.ros.org/urdf/XML/link

URDF: Link – visual – primitives

Geometric primitives for describing visual appearance of the link

```
<link name="base_link">
  <visual>
    <origin xyz="0 0 0.01" rpy="0 0 0"/>
    <geometry>
      <box size="0.2 0.2 0.02"/>
    </geometry>
    <material name="cyan">
      <color rgba="0 1.0 1.0 1.0"/>
    </material>
  </visual>
</link>
```

- Geometric primitives: <box>, <cylinder>, <sphere>
- Materials: <color>, <texture>

URDF: Link – visual – meshes

3D meshes for describing visual appearance of the link

```
<link name="base_link">
  <visual>
    <origin xyz="0 0 0.01" rpy="0 0 0"/>
    <geometry>
      <mesh filename="meshes/base_link.dae"
    </geometry>
  </visual>
  <collision>
     <origin xyz="0 0 0.01" rpy="0 0 0"/>
     <geometry>
          <cylinder radius="1" length="0.5"/>
     </geometry>
  </collision>
</link>
```

- the <collision> element can be simpler from the <visual> in order to reduce computation time

URDF: Link – inertial

Parameters describing the physical properties of the link

```
<link name="base_link">
  <inertial>
    <origin xyz="0 0 0" rpy="0 0 0"/>
    <mass value="1">
    <inertia ixx="100" ixy="0" ixz="0"
             iyy="100" iyz="0" izz="100" />
  </inertial>
</link>
```

- center of gravity `<origin xyz>`
- object mass `<mass value>`
- inertia tensor `<intertia>`

URDF: Inertia

Inertia tensor describes the distribution of mass of the link

- orientation and position of the inertia CS described by <`origin`> tag
- $$ {}^{A}I = \begin{bmatrix} I_{xx} & -I_{xy} & -I_{xz} \\ -I_{xy} & I_{yy} & -I_{yz} \\ -I_{xz} & -I_{yz} & Izz \end{bmatrix} $$
  - diagonal values describe main inertial axes `ixx`, `iyy`, `izz`
  - `ixy`, `ixz`, `iyz` are 0 for symmetric primitives
  - rotations around largest and smallest inertial axis are most stable

URDF: Inertia (cont.)

- moments of inertia:
  $I_{xx} = \int (y^2 + z^2) dm \; I_{yy} = \int (x^2 + z^2) dm \; I_{zz} = \int (x^2 + y^2) dm$

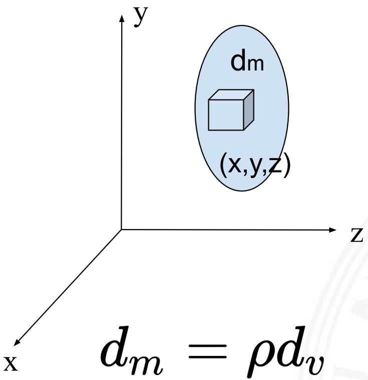

$$d_m = \rho d_v$$

- Products of Inertia:
  $I_{xy} = I_{yx} = \int xydm \; I_{zy} = I_{yz} = \int yzdm \; I_{xz} = I_{zx} = \int zydm$

URDF: Joint

Joint describes geometrical connections of two links.

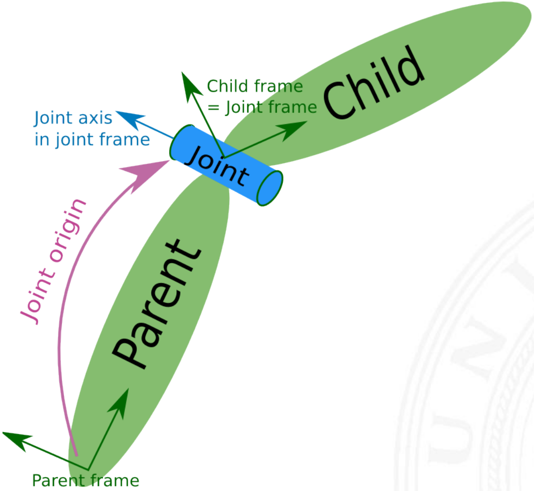

21

URDF: Joint (cont.)

```xml
<joint name="base_link_to_cyl" type="revolute">
  <!-- describes joint position and orientation -->
  <origin xyz="0 0 0.07" rpy="0 0 0"/>

  <!-- describes the related links -->
  <parent link="base_link"/>
  <child link="base_cyl"/>

  <!-- describes the axis of rotation-->
  <axis xyz="0 0 1"/>

  <!-- describes the joint limits-->
  <limit velocity="1.5707963267"
         lower="-3.1415926535" upper="3.1415926535"/>
</joint>
```

[21] http://wiki.ros.org/urdf/XML/joint

URDF: Joint (cont.)

- **type**: revolute, continuous, prismatic, fixed, floating, planar
- **parent_link**: link which the joint is connected to
- **child_link**: link which is connected to the joint
- **axis**: joint axis relative to the joint CS. Represented using a normalized vector
- **limit**: joint limits for motion (lower, upper), velocity and effort
- **dynamics**: damping, friction
- **calibration**: rising, falling
- **mimic**: joint, multiplier, offset
- **safety_controller**: soft_lower_limit, soft_upper_limit, k_position, k_velocity

URDF: Other elements

- sensor
  - position and orientation relative to link
  - sensor properties
    - update rate
    - resolution
    - minimum / maximum angle
- transmissions
  - relation of motor to joint motion
- gazebo
  - simulation properties
- model state
  - description of different robot configurations

Complex Hierachy

Full URDF hierarchy of the TAMS PR2 with the Shadow Hand.

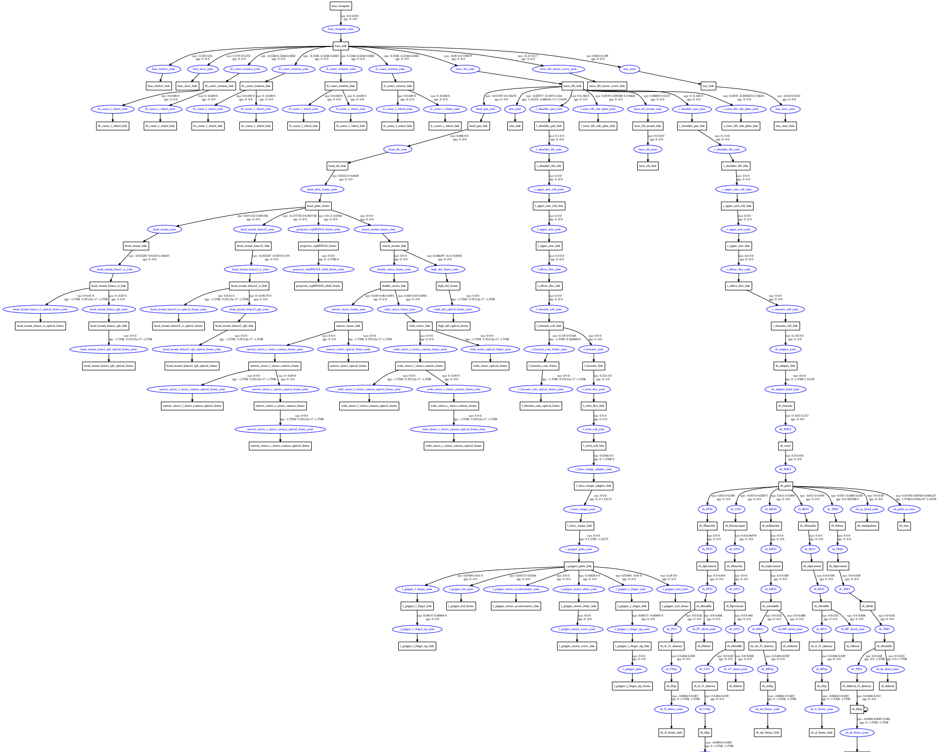
base_footprint
base_footprint_joint
base_link
base_bellow_joint
base_laser_joint
bl_caster_rotation_joint
br_caster_rotation_joint
fl_caster_rotation_joint
fr_caster_rotation_joint
torso_lift_joint
torso_lift_motor_screw_joint
tray_joint
base_bellow_link
base_laser_link
bl_caster_rotation_link
br_caster_rotation_link
fl_caster_rotation_link
fr_caster_rotation_link
torso_lift_link
torso_lift_motor_screw_link
tray_link
bl_caster_l_wheel_joint
bl_caster_r_wheel_joint
br_caster_l_wheel_joint
br_caster_r_wheel_joint
fl_caster_l_wheel_joint
fl_caster_r_wheel_joint
fr_caster_l_wheel_joint
fr_caster_r_wheel_joint
head_pan_joint
imu_joint
l_shoulder_pan_joint
l_torso_lift_side_plate_joint
laser_tilt_mount_joint
r_shoulder_pan_joint
r_torso_lift_side_plate_joint
tray_laser_joint
bl_caster_l_wheel_link
bl_caster_r_wheel_link
br_caster_l_wheel_link
br_caster_r_wheel_link
fl_caster_l_wheel_link
fl_caster_r_wheel_link
fr_caster_l_wheel_link
fr_caster_r_wheel_link
head_pan_link
imu_link
l_shoulder_pan_link
l_torso_lift_side_plate_link
laser_tilt_mount_link
r_shoulder_pan_link
r_torso_lift_side_plate_link
tray_laser_link
head_tilt_joint
l_shoulder_lift_joint
laser_tilt_joint
r_shoulder_lift_joint
head_tilt_link
l_shoulder_lift_link
laser_tilt_link
r_shoulder_lift_link
head_plate_frame_joint
l_upper_arm_roll_joint
r_upper_arm_roll_joint
head_plate_frame
l_upper_arm_roll_link
r_upper_arm_roll_link
head_mount_joint
head_mount_kinect2_joint
projector_wg6802418_frame_joint
sensor_mount_frame_joint
l_upper_arm_joint
r_upper_arm_joint
head_mount_link
head_mount_kinect2_link
projector_wg6802418_frame
sensor_mount_link
l_upper_arm_link
r_upper_arm_link
head_mount_kinect_ir_joint
head_mount_kinect2_ir_joint
projector_wg6802418_child_frame_joint
double_stereo_frame_joint
high_def_frame_joint
l_elbow_flex_joint
r_elbow_flex_joint
head_mount_kinect_ir_link
head_mount_kinect2_ir_link
projector_wg6802418_child_frame
double_stereo_link
high_def_frame
l_elbow_flex_link
r_elbow_flex_link
head_mount_kinect_ir_optical_frame_joint
head_mount_kinect_rgb_joint
head_mount_kinect2_ir_optical_frame_joint
head_mount_kinect2_rgb_joint
narrow_stereo_frame_joint
wide_stereo_frame_joint
high_def_optical_frame_joint
l_forearm_roll_joint
r_forearm_roll_joint
head_mount_kinect_ir_optical_frame
head_mount_kinect_rgb_link
head_mount_kinect2_ir_optical_frame
head_mount_kinect2_rgb_link
narrow_stereo_link
wide_stereo_link
high_def_optical_frame
l_forearm_roll_link
r_forearm_roll_link
head_mount_kinect_rgb_optical_frame_joint
head_mount_kinect2_rgb_optical_frame_joint
narrow_stereo_l_stereo_camera_frame_joint
narrow_stereo_optical_frame_joint
wide_stereo_l_stereo_camera_frame_joint
wide_stereo_optical_frame_joint
l_forearm_cam_frame_joint
l_forearm_joint
rh_adapter_joint
head_mount_kinect_rgb_optical_frame
head_mount_kinect2_rgb_optical_frame
narrow_stereo_l_stereo_camera_frame
narrow_stereo_optical_frame
wide_stereo_l_stereo_camera_frame
wide_stereo_optical_frame
l_forearm_cam_frame
l_forearm_link
rh_adapter_link
narrow_stereo_l_stereo_camera_optical_frame_joint
narrow_stereo_r_stereo_camera_frame_joint
wide_stereo_l_stereo_camera_optical_frame_joint
wide_stereo_r_stereo_camera_frame_joint
l_forearm_cam_optical_frame_joint
l_wrist_flex_joint
rh_adapter_hand_joint
narrow_stereo_l_stereo_camera_optical_frame
narrow_stereo_r_stereo_camera_frame
wide_stereo_l_stereo_camera_optical_frame
wide_stereo_r_stereo_camera_frame
l_forearm_cam_optical_frame
l_wrist_flex_link
rh_forearm
narrow_stereo_r_stereo_camera_optical_frame_joint
wide_stereo_r_stereo_camera_optical_frame_joint
l_wrist_roll_joint
rh_WRJ2
narrow_stereo_r_stereo_camera_optical_frame
wide_stereo_r_stereo_camera_optical_frame
l_wrist_roll_link
rh_wrist
l_force_torque_adapter_joint
rh_WRJ1
l_force_torque_adapter_link
rh_palm
rh_FFJ4
rh_LFJ5
rh_MFJ4
rh_RFJ4
rh_THJ5
rh_ee_fixed_joint
rh_palm_to_imu
l_force_torque_joint
rh_ffknuckle
rh_lfmetacarpal
rh_mfknuckle
rh_rfknuckle
rh_thbase
rh_manipulator
rh_imu
l_force_torque_link
rh_FFJ3
rh_LFJ4
rh_MFJ3
rh_RFJ3
rh_THJ4
l_gripper_palm_joint
rh_ffproximal
rh_lfknuckle
rh_mfproximal
rh_rfproximal
rh_thproximal
l_gripper_palm_link
rh_FFJ2
rh_LFJ3
rh_MFJ2
rh_RFJ2
rh_THJ3
l_gripper_l_finger_joint
l_gripper_led_joint
l_gripper_motor_accelerometer_joint
l_gripper_motor_slider_joint
l_gripper_r_finger_joint
l_gripper_tool_joint
rh_ffmiddle
rh_lfproximal
rh_mfmiddle
rh_rfmiddle
rh_thhub
l_gripper_l_finger_link
l_gripper_led_frame
l_gripper_motor_accelerometer_link
l_gripper_motor_slider_link
l_gripper_r_finger_link
l_gripper_tool_frame
rh_FFJ1
rh_FF_distal_joint
rh_LFJ2
rh_MFJ1
rh_MF_distal_joint
rh_RFJ1
rh_RF_distal_joint
rh_THJ2
l_gripper_l_finger_tip_joint
l_gripper_motor_screw_joint
l_gripper_r_finger_tip_joint
rh_ff_J1_dummy
rh_ffdistal
rh_lfmiddle
rh_mf_J1_dummy
rh_mfdistal
rh_rf_J1_dummy
rh_rfdistal
rh_thmiddle
l_gripper_l_finger_tip_link
l_gripper_motor_screw_link
l_gripper_r_finger_tip_link
rh_FFtip
rh_LFJ1
rh_LF_distal_joint
rh_MFtip
rh_RFtip
rh_THJ1
rh_th_distal_joint
l_gripper_joint
rh_fftip
rh_lf_J1_dummy
rh_lfdistal
rh_mftip
rh_rftip
rh_thdistal_J1_dummy
rh_thdistal
l_gripper_l_finger_tip_frame
rh_ff_biotac_joint
rh_LFtip
rh_mf_biotac_joint
rh_rf_biotac_joint
rh_thtip
rh_ff_biotac_link
rh_lftip
rh_mf_biotac_link
rh_rf_biotac_link
rh_th_biotac_joint

Outline

Outline (cont.)

Inverse kinematics for manipulators

- **Forward Kinematics**: given robot configurations(joint angles), find position & orientations of the end-effector

Set of problems

- In the majority of cases the control of robot manipulators takes place in the *joint space*,
- The informations about objects are mostly given in the *cartesian space*.

- **Inverse Kinematics**: give position & orientations of the end-effector, find robot configurations(joint angles)

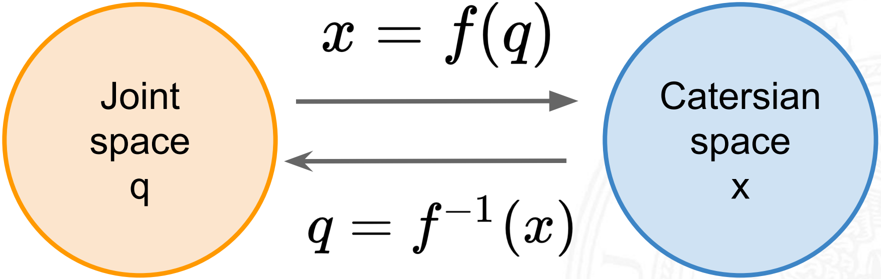

Existence of solutions: Workspace

Workspace: the volume of space that is reachable for the tool of the manipulator.

- reachable workspace
- dexterous workspace

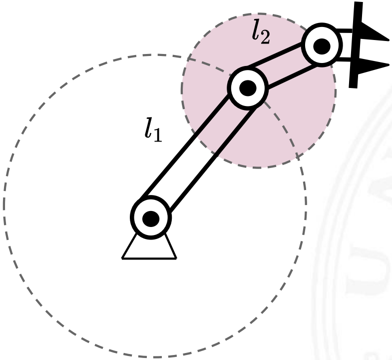

Existence of solutions: Workspace (cont.)

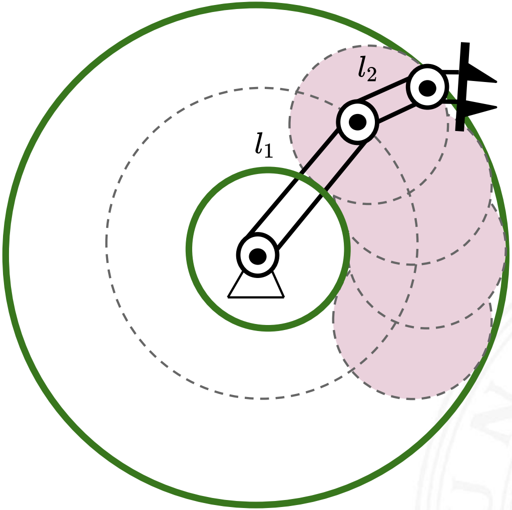

if $l_1 \neq l_2$, the reachable workspace becomes a ring of outer radius $|l_1 + l_2|$,and inner radius $|l_1 - l_2|$.

Existence of solutions: Workspace (cont.)

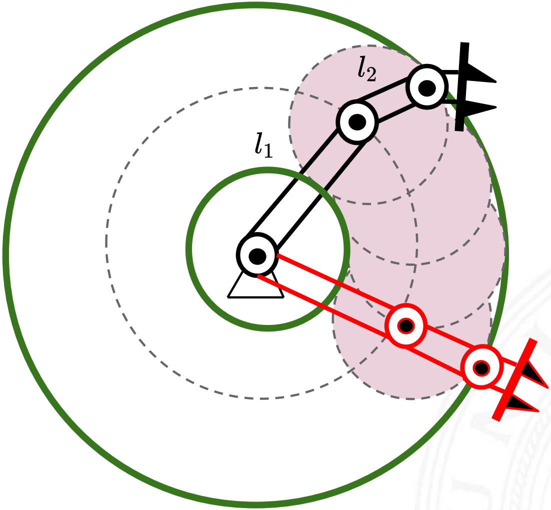

Does the workspace change if joint limits are considered?
For example, $q_1 \in [0, \pi], q_2 \in [0, \pi]$.

Multiple solutions

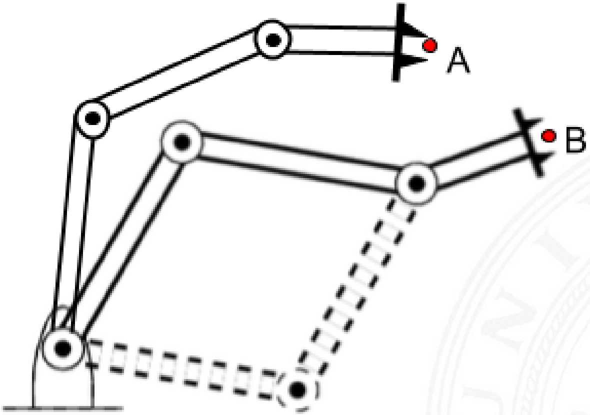

The solution using the example of PUMA 560

$$T_6 = T' T'' = \begin{bmatrix} n_x & o_x & a_x & p_x \\ n_y & o_y & a_y & p_y \\ n_z & o_z & a_z & p_z \\ 0 & 0 & 0 & 1 \end{bmatrix}$$

where

$$n_x = C_1[C_{23}(C_4 C_5 C_6 - S_4 S_6) - S_{23} S_5 C_6] - S_1(S_4 C_5 C_6 + C_4 S_6) \quad (2)$$

$$n_y = S_1[C_{23}(C_4 C_5 C_6 - S_4 S_6 - S_{23} S_5 S_6] + C_1(S_4 C_5 C_6 + C_4 S_6) \quad (3)$$

$$n_z = -S_{23}[C_4 C_5 C_6 - S_4 S_6] - C_{23} S_5 C_6 \quad (4)$$

The solution using the example of PUMA 560 (cont.)

$$o_x = \ldots \tag{5}$$

$$o_y = \ldots \tag{6}$$

$$o_z = \ldots \tag{7}$$

$$a_x = \ldots \tag{8}$$

$$a_y = \ldots \tag{9}$$

$$a_z = \ldots \tag{10}$$

$$p_x = C_1[d_6(C_{23}C_4S_5 + S_{23}C_5) + S_{23}d_4 + a_3C_{23} + a_2C_2] - S_1(d_6S_4S_5 + d_2) \tag{11}$$

$$p_y = S_1[d_6(C_{23}C_4S_5 + S_{23}C_5) + S_{23}d_4 + s_3C_{23} + a_2C_2] + C_1(d_6S_4S_5 + d_2) \tag{12}$$

$$p_z = d_6(C_{23}C_5 - S_{23}C_4S_5) + C_{23}d_4 - a_3S_{23} - a_2S_2 \tag{13}$$

Remark

- Non-linear equations
- Existence of solutions
- Multiple solutions
- `Different solution strategy:` closed solutions vs. numerical solutions

Different methods for solution finding

Closed form (analytical):
An expression is said to be a closed-form experession if it can be expressed analytically in terms of a bounded number of certain 'well-known' functions.

- $+ - \times \div$
- nth roots
- exponent and logarithm
- trigonometric and inverse trigonometric functions
- Do not include infinite series, continued fractions, integrals or limits.

Different methods for solution finding (cont.)

Closed form (analytical):

- `algebraic solution`
  - + accurate solution by means of equations
  - – solution is not geometrically representative
- `geometrical solution`
  - + case-by-case analysis of possible robot configurations
  - – robot specific

Numerical form:

- `iterative methods`
  - + the methods are transferable
  - – computationally intensive, for several exceptions the convergence can not be guaranteed

Algebraic solution

Algebraic Approach manipulates the given equations into a form whose solution is known.

- Method1: **Transcendental equations**

$1.\ \sin\theta = a \Rightarrow \theta = A\tan 2(a, \pm\sqrt{1-a^2})$

$2.\ \cos\theta = b \Rightarrow \theta = \pm A\tan 2(\sqrt{1-b^2}, b)$

$3.\begin{cases} \sin\theta = a \\ \cos\theta = b \end{cases} \Rightarrow \theta = A\tan 2(a, b)$

$4.\ a\cos\theta + b\sin\theta = 0 \Rightarrow \theta = A\tan 2(a, -b)\ or\ \theta = A\tan 2(-a, b)$

$5.\ a\cos\theta + b\sin\theta = c \Rightarrow \theta = A\tan 2(b, a) \pm A\tan 2(\sqrt{a^2+b^2-c^2}, c)$

$6.\begin{cases} a\cos\theta - b\sin\theta = c \\ a\sin\theta + b\cos\theta = d \end{cases} \Rightarrow \theta = A\tan 2(ad - ba, ac - bd)$

Algebraic solution (cont.)

We define the function *Atan*2 as:

$$\theta = Atan2(y,x) = \begin{cases} Atan(\frac{y}{x}) & \text{for } +x \\ Atan(\frac{y}{x}) + \pi & \text{for } -x, +y_0 \\ Atan(\frac{y}{x}) - \pi & \text{for } -x, -y \\ \frac{\pi}{2} & \text{for } x = 0, +y \\ \frac{-\pi}{2} & \text{for } x = 0, -y \\ NaN & \text{for } x = 0, y = 0 \end{cases}$$

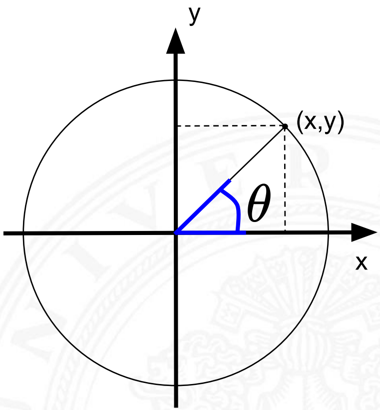

Algebraic solution (cont.)

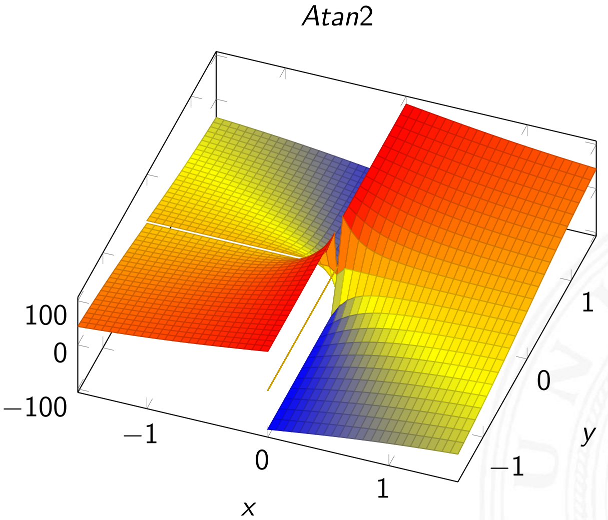

Example: a planar 3 DOF manipulator

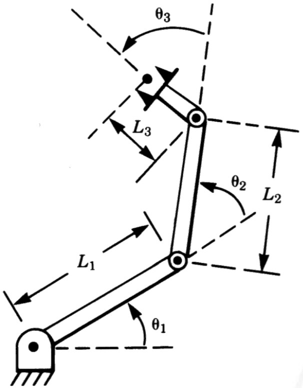

Joint	α_{i-1}	a_{i-1}	d_i	θ_i
1	0	0	0	θ_1
2	0	l_1	0	θ_2
3	0	l_2	0	θ_3

The algebraical solution for the 3 DOF planar

$$T_6 = {}^0T_3 = \begin{bmatrix} C_{123} & -S_{123} & 0 & l_1 C_1 + l_2 C_{12} \\ S_{123} & C_{123} & 0 & l_1 S_1 + l_2 S_{12} \\ 0 & 0 & 1 & 0 \\ 0 & 0 & 0 & 1 \end{bmatrix}$$

with $C_{ij[k]} = \cos(\theta_i + \theta_j[+\theta_k])$

Specification for the TCP: (x, y, ϕ). For such kind of vectors applies:

$${}^0T_3 = \begin{bmatrix} C_\phi & -S_\phi & 0 & x \\ S_\phi & C_\phi & 0 & y \\ 0 & 0 & 1 & 0 \\ 0 & 0 & 0 & 1 \end{bmatrix}$$

The algebraical solution for the 3 DOF planar (cont.)

Resultant, four equations can be derived:

$$C_\phi = C_{123} \tag{14}$$

$$S_\phi = S_{123} \tag{15}$$

$$x = l_1 C_1 + l_2 C_{12} \tag{16}$$

$$y = l_1 S_1 + l_2 S_{12} \tag{17}$$

The algebraical solution for the 3 DOF planar (cont.)

Square and add (20) ($x = l_1 C_1 + l_2 C_{12}$) and (21) ($y = l_1 S_1 + l_2 S_{12}$)

$$x^2 + y^2 = l_1^1 + l_2^2 + 2 l_1 l_2 C_2$$

using

$$C_{12} = C_1 C_2 - S_1 S_2, S_{12} = C_1 S_2 + S_1 C_2$$

giving

$$C_2 = \frac{x^2 + y^2 - l_1^2 - l_2^2}{2 l_1 l_2}$$

for goal in workspace

$$S_2 = \pm\sqrt{1 - C_2^2}$$

solution

$$\theta_2 = atan2(S_2, C_2)$$

The algebraical solution for the 3 DOF planar (cont.)

solve (20) $(x = l_1 C_1 + l_2 C_{12})$ and (21) $(y = l_1 S_1 + l_2 S_{12})$ for θ_1

$$\theta_1 = atan2(y, x) - atan2(k_2, k_1)$$

where $k_1 = l_1 + l_2 C_2$ and $k_2 = l_2 S_2$.

solve θ_3 from (19) $(C_\phi = C_{123})$ and (18) $(S_\phi = S_{123})$

$$\theta_1 + \theta_2 + \theta_3 = atan2(S_\phi, C_\phi) = \phi$$

Analytical solvability of manipulator

The closed solution exists if specific constraints (sufficient constraints) for the arm geometry are satisfied:

`If` 3 sequent axes intersect in a given point

`or if` 3 sequent axes are parallel to each other

- manipulators should be designed regarding these constraints
- most of them are
  - PUMA 560: axes 4, 5 & 6 intersect in a single point
  - Mitsubishi PA10, KUKA LWR, PR2
  - 3-DOF planar (RPC)

Algebraical solution (polynomial conversion)

Method2: **Reduction to polynomial**

The following substitutions are used for the polynomial conversion of transcendental equations:

$$u = tan\frac{\theta}{2}$$

$$\cos\theta = \frac{1-u^2}{1+u^2}$$

$$\sin\theta = \frac{2u}{1+u^2}$$

Algebraical solution (polynomial conversion) (cont.)

Example:
The following transcendental equation is given:

$$a\cos\theta + b\sin\theta = c$$

$\Rightarrow \theta = A\tan 2(b, a) \pm A\tan 2(\sqrt{a^2 + b^2 - c^2}, c)$
After the polynomial conversion:

$$a(1 - u^2) + 2bu = c(1 + u^2)$$

The solution for u:

$$u = \frac{b \pm \sqrt{b^2 - a^2 - c^2}}{a + c}$$

Then:

$$\theta = 2tan^{-1}(\frac{b \pm \sqrt{b^2 - a^2 - c^2}}{a + c})$$

Geometrical solution

- Decompose the spatial geometry of the arm into several plane geometry problems
- Law of cosines: $c^2 = a^2 + b^2 - 2ab\cos\alpha$

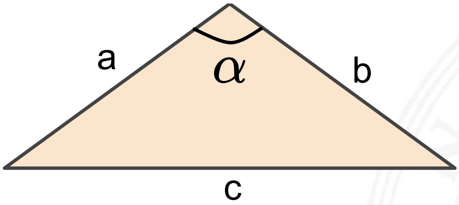

The geometrical solution for the example 1

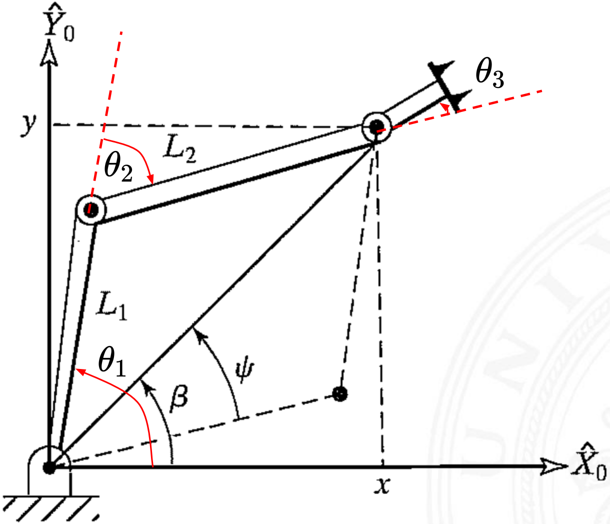

The geometrical solution for the example 1 (cont.)

Calculate θ_2 via the `law of cosines`:

$$x^2 + y^2 = l_1^2 + l_2^2 - 2 l_1 l_2 \cos(180 + \theta_2)$$

The solution:

$$\theta_2 = \pm cos^{-1} \frac{x^2 + y^2 - l_1^2 - l_2^2}{2 l_1 l_2}$$

$$\theta_1 = \beta \pm \psi$$

where:

$$\beta = atan2_m(y, x), \quad \cos\psi = \frac{x^2 + y^2 - l_1^2 - l_2^2}{2 l_1 \sqrt{x^2 + y^2}}$$

For $\theta_1, \theta_2, \theta_3$ applies:

$$\theta_1 + \theta_2 + \theta_3 = \phi$$

Exercise

Assume we have derived the forward kinematics as:

$$
{}^0T_3 = \begin{bmatrix} C_1 C_{23} & -C_1 S_{23} & S_1 & C_1(C_2 l_2 + l_1) \\ S_1 C_{23} & -S_1 S_{23} & -C_1 & S_1(C_2 l_2 + l_1) \\ S_{23} & C_{23} & 0 & S_2 l_2 \\ 0 & 0 & 0 & 1 \end{bmatrix}
$$

And we know:

$$
{}^0T_3 = \begin{bmatrix} r_{11} & r_{12} & r_{13} & p_x \\ r_{21} & r_{22} & r_{23} & p_y \\ r_{31} & r_{32} & r_{33} & p_z \\ 0 & 0 & 0 & 1 \end{bmatrix}
$$

Question: How to solve the inverse kinematics?

IKFast

- Closed-form solutions
- OpenRAVE
- faster (4 μs) but only work with any number of joints arranged in a chain
- Tutorial: ikfast MoveIt! kinematics_base plugin

TracIK

- TRACLabs' IK solver
- Tutorial: trac_ik MoveIt! kinematics_base plugin
- two IK implementations:
  KDL's Newton-based convergence algorithm
  SQP (Sequential Quadratic Programming) nonlinear optimization approach
- trac_ik_python (RPC)

BioIk

BioIK 1

KDL

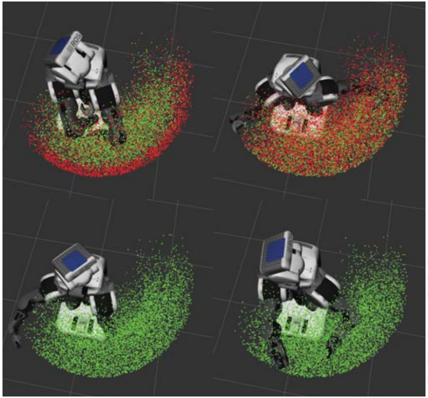

TrackIK

BioIK 2

Download link: bio_ik MoveIt! kinematics_base plugin
22

[22] Ruppel, P., Hendrich, N., Starke, S. and Zhang, J., 2018, May. Cost functions to specify full-body motion and multi-goal manipulation tasks. In 2018 ICRA (pp. 3152-3159). IEEE.

Bibliography

[1] G.-Z. Yang, R. J. Full, N. Jacobstein, P. Fischer, J. Bellingham, H. Choset, H. Christensen, P. Dario, B. J. Nelson, and R. Taylor, "Ten robotics technologies of the year," 2019.

[2] J. K. Yim, E. K. Wang, and R. S. Fearing, "Drift-free roll and pitch estimation for high-acceleration hopping," in *2019 International Conference on Robotics and Automation (ICRA)*, pp. 8986–8992, IEEE, 2019.

[3] J. F. Engelberger, *Robotics in service*.
MIT Press, 1989.

[4] K. Fu, R. González, and C. Lee, *Robotics: Control, Sensing, Vision, and Intelligence*.
McGraw-Hill series in CAD/CAM robotics and computer vision, McGraw-Hill, 1987.

[5] R. Paul, *Robot Manipulators: Mathematics, Programming, and Control: the Computer Control of Robot Manipulators*.
Artificial Intelligence Series, MIT Press, 1981.

[6] J. Craig, *Introduction to Robotics: Pearson New International Edition: Mechanics and Control*.
Always learning, Pearson Education, Limited, 2013.

Bibliography (cont.)

[7] T. Flash and N. Hogan, "The coordination of arm movements: an experimentally confirmed mathematical model," *Journal of neuroscience*, vol. 5, no. 7, pp. 1688–1703, 1985.

[8] T. Kröger and F. M. Wahl, "Online trajectory generation: Basic concepts for instantaneous reactions to unforeseen events," *IEEE Transactions on Robotics*, vol. 26, no. 1, pp. 94–111, 2009.

[9] W. Böhm, G. Farin, and J. Kahmann, "A Survey of Curve and Surface Methods in CAGD," *Comput. Aided Geom. Des.*, vol. 1, pp. 1–60, July 1984.

[10] J. Zhang and A. Knoll, "Constructing Fuzzy Controllers with B-spline Models - Principles and Applications," *International Journal of Intelligent Systems*, vol. 13, no. 2-3, pp. 257–285, 1998.

[11] M. Eck and H. Hoppe, "Automatic Reconstruction of B-spline Surfaces of Arbitrary Topological Type," in *Proceedings of the 23rd Annual Conference on Computer Graphics and Interactive Techniques*, SIGGRAPH '96, (New York, NY, USA), pp. 325–334, ACM, 1996.

Bibliography (cont.)

[12] A. Cowley, W. Marshall, B. Cohen, and C. J. Taylor, "Depth space collision detection for motion planning," 2013.

[13] Hornung, Armin and Wurm, Kai M. and Bennewitz, Maren and Stachniss, Cyrill and Burgard, Wolfram, "OctoMap: an efficient probabilistic 3D mapping framework based on octrees," *Autonomous Robots*, vol. 34, pp. 189–206, 2013.

[14] D. Berenson, S. S. Srinivasa, D. Ferguson, and J. J. Kuffner, "Manipulation planning on constraint manifolds," in *2009 IEEE International Conference on Robotics and Automation*, pp. 625–632, 2009.

[15] S. Karaman and E. Frazzoli, "Sampling-based algorithms for optimal motion planning," *The International Journal of Robotics Research*, vol. 30, no. 7, pp. 846–894, 2011.

[16] O. Khatib, "The Potential Field Approach and Operational Space Formulation in Robot Control," in *Adaptive and Learning Systems*, pp. 367–377, Springer, 1986.

[17] L. E. Kavraki, P. Svestka, J. Latombe, and M. H. Overmars, "Probabilistic roadmaps for path planning in high-dimensional configuration spaces," *IEEE Transactions on Robotics and Automation*, vol. 12, no. 4, pp. 566–580, 1996.

Bibliography (cont.)

[18] J. Kuffner and S. LaValle, "RRT-Connect: An Efficient Approach to Single-Query Path Planning.," vol. 2, pp. 995–1001, 01 2000.

[19] J. Starek, J. Gómez, E. Schmerling, L. Janson, L. Moreno, and M. Pavone, "An asymptotically-optimal sampling-based algorithm for bi-directional motion planning," *Proceedings of the ... IEEE/RSJ International Conference on Intelligent Robots and Systems. IEEE/RSJ International Conference on Intelligent Robots and Systems*, vol. 2015, 07 2015.

[20] D. Hsu, J. . Latombe, and R. Motwani, "Path planning in expansive configuration spaces," in *Proceedings of International Conference on Robotics and Automation*, vol. 3, pp. 2719–2726 vol.3, 1997.

[21] A. H. Qureshi, A. Simeonov, M. J. Bency, and M. C. Yip, "Motion planning networks," in *2019 International Conference on Robotics and Automation (ICRA)*, pp. 2118–2124, IEEE, 2019.

[22] J. Schulman, J. Ho, A. Lee, I. Awwal, H. Bradlow, and P. Abbeel, "Finding locally optimal, collision-free trajectories with sequential convex optimization," in *in Proc. Robotics: Science and Systems*, 2013.

Bibliography (cont.)

[23] A. T. Miller and P. K. Allen, "Graspit! a versatile simulator for robotic grasping," *IEEE Robotics Automation Magazine*, vol. 11, no. 4, pp. 110–122, 2004.

[24] A. ten Pas, M. Gualtieri, K. Saenko, and R. Platt, "Grasp pose detection in point clouds," *The International Journal of Robotics Research*, vol. 36, no. 13-14, pp. 1455–1473, 2017.

[25] L. P. Kaelbling and T. Lozano-Pérez, "Hierarchical task and motion planning in the now," in *2011 IEEE International Conference on Robotics and Automation*, pp. 1470–1477, 2011.

[26] N. T. Dantam, Z. K. Kingston, S. Chaudhuri, and L. E. Kavraki, "Incremental task and motion planning: A constraint-based approach.," in *Robotics: Science and Systems*, pp. 1–6, 2016.

[27] J. Ferrer-Mestres, G. Francès, and H. Geffner, "Combined task and motion planning as classical ai planning," *arXiv preprint arXiv:1706.06927*, 2017.

[28] M. Görner, R. Haschke, H. Ritter, and J. Zhang, "MoveIt! Task Constructor for Task-Level Motion Planning," in *IEEE International Conference on Robotics and Automation (ICRA)*, 2019.

[29] K. Hauser and J.-C. Latombe, "Multi-modal motion planning in non-expansive spaces," *The International Journal of Robotics Research*, vol. 29, no. 7, pp. 897–915, 2010.

[30] B. Siciliano and O. Khatib, *Springer handbook of robotics*. Springer, 2016.

[31] P. Sermanet, C. Lynch, Y. Chebotar, J. Hsu, E. Jang, S. Schaal, S. Levine, and G. Brain, "Time-contrastive networks: Self-supervised learning from video," in *2018 IEEE International Conference on Robotics and Automation (ICRA)*, pp. 1134–1141, IEEE, 2018.

[32] C. Finn, P. Abbeel, and S. Levine, "Model-agnostic meta-learning for fast adaptation of deep networks," *arXiv preprint arXiv:1703.03400*, 2017.

[33] R. Brooks, "A robust layered control system for a mobile robot," *Robotics and Automation, IEEE Journal of*, vol. 2, pp. 14–23, Mar 1986.

[34] M. J. Mataric, "Interaction and intelligent behavior.," tech. rep., DTIC Document, 1994.

Bibliography (cont.)

[35] M. P. Georgeff and A. L. Lansky, "Reactive reasoning and planning.," in *AAAI*, vol. 87, pp. 677–682, 1987.

[36] J. S. Albus, "The nist real-time control system (rcs): an approach to intelligent systems research," *Journal of Experimental & Theoretical Artificial Intelligence*, vol. 9, no. 2-3, pp. 157–174, 1997.

[37] T. Fukuda and T. Shibata, "Hierarchical intelligent control for robotic motion by using fuzzy, artificial intelligence, and neural network," in *Neural Networks, 1992. IJCNN., International Joint Conference on*, vol. 1, pp. 269–274 vol.1, Jun 1992.

[38] L. Einig, *Hierarchical Plan Generation and Selection for Shortest Plans based on Experienced Execution Duration*.
Master thesis, Universität Hamburg, 2015.

[39] J. Craig, *Introduction to Robotics: Mechanics & Control. Solutions Manual*.
Addison-Wesley Pub. Co., 1986.

Bibliography (cont.)

[40] H. Siegert and S. Bocionek, *Robotik: Programmierung intelligenter Roboter: Programmierung intelligenter Roboter*. Springer-Lehrbuch, Springer Berlin Heidelberg, 2013.

[41] R. Schilling, *Fundamentals of robotics: analysis and control*. Prentice Hall, 1990.

[42] T. Yoshikawa, *Foundations of Robotics: Analysis and Control*. Cambridge, MA, USA: MIT Press, 1990.

[43] M. Spong, *Robot Dynamics And Control*. Wiley India Pvt. Limited, 2008.